Fractional Order Simulation of MHD Blood flow with radiation and reaction effects.

[1*]Harshad Patel, [2]Snehal Patel, [3]Nilesh Patel,

[1*, 2]. U. V.Patel College of Engineering,
Ganpat University,Mehsana, India
[3]B. S. P. P. Ganpat University, Mehsana, India

Corresponding Author: **Harshad Patel** [1*]
Email: [1*] harshadpatel2@gmail.com

Abstract

Unsteady MHD Casson blood flow in porous media: impacts of radiation, chemical reactions, thermos-diffusion, and heat generation are discussed in this study. An example of a bio viscosity non-Newtonian fluid with an inclination angle and a vibration mode is blood. A dimensionless form of the governing equations is achieved by use of the similarity transformation. The governing equations are subjected to the Caputo-Fabrizio fractional ordered derivative in order to increase the influence of the physical viewpoint. The precise formulation of concentration profiles, energies, and momentum is determined by applying the Laplace and Finite Hankel transforms. The consequences of various physical parameters are illustrated through graphs for a better understanding.

Keywords: Magnetic field; Thermal diffusion; Casson fluid; Thermal radiation; fractional derivative;

Nomenclature:

β_0 Uniform magnetic field

B_0 Systolic Pressure gradient

B_1 Diastolic Pressure gradient

θ_m Metabolic Heat absorption

u Velocity

β Casson fluid parameter

r Radial coordinator

$\emptyset_0$ Phase angle

ω Pulsatile frequency

C Concentration

μ_B Plastic dynamic viscosity

θ Temperature

τ_r Yield stress

C_p Specific heat at constant pressure

$2\pi_c$ A critical value of this model

Sc Schmidt number

F Inclination angle parameter

S_c Schmidt number

M Magnetic parameter

P Oscillating pressure gradient

t Dimensionless time

Q_m Metabolic Heat Source

R_e Reynolds Number

C_p Specific heat at constant pressure

P_e Peclet Number

Sr Soret Number

D_M Mass diffusion coefficient

Gm Mass Grashof number

Gr Thermal Grashof number

Nr Thermal Radiation

Kc Chemical Reaction

Pr Prandtl number

Greek symbols:

υ Kinematic viscosity coefficient

β_T Volumetric thermal expansion coefficient

β_c Volumetric concentration expansion coefficient

ρ Fluid density

g Acceleration due to gravity

σ Electrical conductivity

K_1 Thermal conductivity

1. Introduction:

Non-Newtonian fluids include some materials with significant commercial applications that don't display Newtonian fluid behaviour. It is important to note that the subclass of non-Newtonian fluid and the amount of shear stress exerted on it significantly affect how the fluid behaves. One basic model for non-Newtonian fluids is the Casson fluid which is introduced by Casson [1]. The Casson fluid model to forecast how pigment-oil suspensions would behave in terms of their flow characteristics. Human blood can also be considered a Casson fluid. Batchelor and George [2] is credited with being the first person to revolutionise the boundary layer behaviour of a continuously extending surface. Pramanik [3] studied Casson fluid flow is flowing exponentially with heat transfer effects. Study of Casson flow in temperature-dependent walls done by Bhattacharyya et al. [4], who found an accurate solution for the thermal boundary layer. Mahanta and Shaw [5] considered 3D Casson blood flow past in linear extending sheet. Wall shear stress on unsteady MHD flow with heat and mass transfer effects explored by Alie al. [6]. However, Kataria and Patel [7] investigated a Casson fluid flow through a porous media while accounting for MHD effects, heat radiation, and chemical reactions. In this analysis, we assume that the thermal radiation impact is linear. Kataria and Patel [8] studied a vertically vibrating plate in an isothermal condition, mixed convection flow with a ramping wall temperature. Since the fluid's temperature is affected by the boundary conditions, it would change with time (t). On the other hand, Shukla et al. [9] looked at the effects of an MHD effect, radiation absorption, and heat production or absorption on the behaviour of a Casson fluid. Unsteady free convective MHD Casson fluid flow has been examined under a variety of situations by researchers including Nadeem [10] and Shehzad [11]. Understanding how a magnetic field, thermal diffusion, and acceleration of the body affect blood flow at the fractional-order derivative level is a novel and interesting research topic. Leibniz introduced the idea of a derivative of a fractional order in 1695, and Liouville developed this concept further in 1832. Time derivatives of fractional orders have found useful applications in a wide variety of disciplines, from fluid mechanics to biology to mathematics to economics, etc. The velocity of blood and magnetic particles was slowed by an external magnetic field, as predicted by Caputo fractional derivatives, Laplace, and finite Hankel transforms. Some of the most widely used definitions to this day are those of Riemann-Liouville, Grunwald-Letnikov, and Caputo [12] Recently, Atangana and Ilknu [13] published one of the most up-to-date definitions of a fractional derivative. In their expanded work, Sheikh et al. [14] accounted for the results of a chemical reaction, heat absorption, and heat production.

The current research replicated the previous one, establishing the same conclusion on the behaviour of fluids with varying fractional definitions. Maiti et al. [15] investigated the heat and mass transport of a Casson fluid via a porous cylindrical tube under the influence of magnetohydrodynamic (MHD) and thermal radiation. The scientists investigated how a magnetic field and thermal radiation affect heat and mass transfer in an accelerated arterial segment. Jamil et al. [16] conducted a study on the flow of non-Newtonian magnetic Casson blood in an inclined stenosed artery. They utilized Caputo-Fabrizio fractional derivatives in their analysis. The numerical flow of a non-Newtonian fluid through an axisymmetric stenosis was investigated by Nakamura et al. [17]. Sud and Sekhon [18] discussed flow in a stenosed artery. The fractional derivative concepts are very important role in engineering applications. Recently, many researchers considered fractional time derivative model in fluid flow problems [19-21]. Ramesh and Devakar [22] obtained analytical results of Casson fluid flow problems whereas, Akbar [23] studied blood flow problems with Prandtl fluid model in tapered stenosed arteries. The work of MHD flow of Casson fluid with different physical and boundary conditions done by Kataria and Patel [24] and Mittal et al. [25].

After going over the literature review that was indicated before, we came to the conclusion that the impacts of thermal radiation, chemical reaction, thermos-diffusion, and heat generation were not specifically discussed on unsteady MHD Casson blood flow in porous medium. To determine the precise expression of momentum, energy, and concentration profiles, the Laplace transform and the finite Hankel transform are utilized.

Mathematical Formulation:

Let us consider thermal radiation, chemical reaction, thermos-diffusion and heat generation effects on unsteady free convective Casson Blood flow in the presence of magnetic field with periodic vibration. The focus of the current research is on unsteady fluid flow in artery, which is outlined in Figure 1 and $z-axis$ is axial direction, while $r-axis$ indicates radial direction. An oscillating pressure gradient was utilized to create a non-Newtonian Casson fluid, which was subsequently used as a model for blood (Jamil et al. [16]). Blood flow can be increased by applying a magnetic field B_0 perpendicular to the z-axis. The induced magnetic field is not taken into consideration over the course of this endeavour. Both laminar flow and unstable free convection flow are characteristics of our flow behaviour. Due to the fact that we are unable to take into account the force convection phenomenon, it is impossible for us to extend our study to include both turbulent and steady flow.

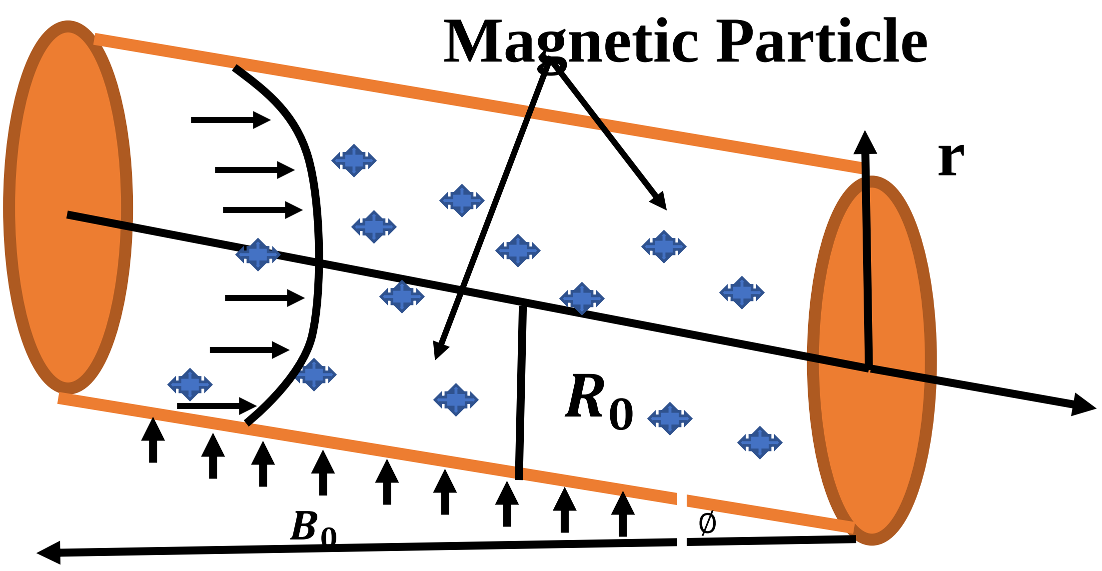

Figure 1: Physical Sketch of the Problem

The constitutive equations of bio viscosity rheology of Casson fluid model gives Nakamura and Sawada [17]

$$\tau_{ij} = \begin{cases} 2\left(\mu B + \frac{Py}{\sqrt{2\pi}}\right) e_{ij} & \pi > \pi_c \\ 2\left(\mu B + \frac{Py}{\sqrt{2\pi_c}}\right) e_{ij} & \pi < \pi_c \end{cases} \tag{1}$$

In this formula μ_B is the plastic dynamic viscosity, P_y is fluid's yield stress, $\pi = \left(e_{ij}\right)^2$ where e_{ij} is the deformation rate of the $(i,i)^{th}$ component. π_c is the critical value of π.

In the equation (1) P_y is given by

$$P_y = \frac{\mu\, B\, \sqrt{2\pi}}{\gamma} \tag{2}$$

According to the Batchelor's [2] viscosity for the Newtonian system is written as,

$$\tau^* = \mu\, \frac{\partial u}{\partial y} \tag{3}$$

For the Non-Newtonian Casson fluid flow, we consider $\pi > \pi_c$.

$$\mu = \mu_B + \frac{P_y}{\sqrt{2\pi}} \tag{4}$$

As a result, the induced magnetic fields can be disregarded and the magnetic Reynolds numbers can be very minimal. Under above assumptions, the governing equations can be written as,

$$\rho \frac{\partial u}{\partial t} = -\frac{\partial p}{\partial z} + \mu \left(1 + \frac{1}{\beta}\right)\left(\frac{\partial^2 u}{\partial r^2} + \frac{1}{r}\frac{\partial u}{\partial r}\right) + G(t) - \frac{\mu}{k}u - \sigma {\beta_0}^2 sin\theta_1\, u + g\beta_T(T - T_w) + g\beta_C(C - C_w) + gsin\emptyset \quad (5)$$

$$\frac{\partial T}{\partial t} = \frac{K_1}{\rho C_p}\left(\frac{\partial^2 T}{\partial r^2} + \frac{1}{r}\frac{\partial T}{\partial r}\right) - \frac{1}{\rho C_p}\frac{\partial q}{\partial r} + \frac{Q_m + \theta_m}{\rho C_p} \quad (6)$$

$$\frac{\partial C}{\partial t} = D_m\left(\frac{\partial^2 C}{\partial r^2} + \frac{1}{r}\frac{\partial C}{\partial r}\right) + \frac{D_m K_T}{T_\infty}\left(\frac{\partial^2 T}{\partial r^2} + \frac{1}{r}\frac{\partial T}{\partial r}\right) - K_2(C - C_\infty) \quad (7)$$

The periodic vibration term, $G(t)$ which is appear in equation (5) can be put mathematically Sud et al. [18] as,

$$G(t) = A_0 Cos(Kt + \emptyset_0) \quad (8)$$

The pressure gradient can be express mathematically as,

$$-\frac{\partial p}{\partial z} = B_0 + B_1\cos(\omega t) \quad (9)$$

with I.C. and B.C.

$$u = T = C = 0 \; at \; t = 0, \forall r \in [0, R_0] \quad (10)$$

$$\frac{\partial u}{\partial r} = \frac{\partial T}{\partial r} = \frac{\partial C}{\partial r} = 0, at \; r = 0, t > 0 \quad (11)$$

$$u = 0, T = T_w, C = C_w \; at \; r = 1, t > 0 \quad (12)$$

By introducing following similarity transformations, the set of revised form of governing equations which are dimensionless are as under.

$$r^* = \frac{r}{R_0},\; t^* = \frac{tu_0}{R_0},\; u^* = \frac{u}{u_0},\; p^* = \frac{p}{\rho {u_0}^2},\; z^* = \frac{z}{R_0}, \omega^* = \frac{R_0\omega}{u_0},\; K^* = \frac{K}{u_0}, {A_0}^* = \frac{A_0 R_0}{{u_0}^2}$$

$$\theta = \frac{T - T_\omega}{T_\omega - T_\infty},\quad \emptyset = \frac{C - C_\omega}{C_\omega - C_\infty}, Q_m = \frac{R_0\overline{Q_m}}{u_0\rho c_p(T_\omega - T_\infty)}, \theta_m = \frac{R_0\overline{\theta_m}}{u_0\rho c_p(T_\omega - T_\infty)}, Nr = \frac{4\,\alpha_1^2 R_0^2}{K}$$

In the equations (5-12) dropping out the " $*$ " notation (for simplicity) we get,

$$\frac{\partial u}{\partial t} = B_0 + B_1\cos(\omega t) + \frac{1}{R_e}\left(1 + \frac{1}{\beta}\right)\left(\frac{\partial^2 u}{\partial r^2} + \frac{1}{r}\frac{\partial u}{\partial r}\right) + A_0 Cos(Kt + \emptyset_0) - \frac{1}{D_a R_e}u - \frac{M^2}{R_e}u + \frac{Gr}{{R_e}^2}\theta + \frac{Gm}{{R_e}^2}C + \frac{sin\emptyset}{F} \quad (13)$$

$$P_e\frac{\partial \theta}{\partial t} = \left(\frac{\partial^2 \theta}{\partial r^2} + \frac{1}{r}\frac{\partial \theta}{\partial r}\right) + Nr\theta + P_e(Q_m + \theta_m) \quad (14)$$

$$R_e Sc\,\frac{\partial C}{\partial t} = \left(\frac{\partial^2 C}{\partial r^2} + \frac{1}{r}\frac{\partial C}{\partial r}\right) + Sr\,Sc\,\left(\frac{\partial^2 \theta}{\partial r^2} + \frac{1}{r}\frac{\partial \theta}{\partial r}\right) - S_c K_c R_e^2 C \quad (15)$$

with I.C. and B.C.

$$u = \theta = C = 0 \; at \; t = 0, \forall r \in [0, 1] \tag{16}$$

$$\frac{\partial u}{\partial r} = \frac{\partial \theta}{\partial r} = \frac{\partial C}{\partial r} = 0, at \; r = 0, t > 0 \tag{17}$$

$$u = 0, \theta = 0, C = 0 \; at \; r = 1, t > 0 \tag{18}$$

Where,

$R_e = \frac{R_0 u_0}{\nu}, D_a = \frac{k}{{R_0}^2}, M^2 = \frac{\sigma B_0^2 {R_0}^2}{\rho \nu} sin\theta_1, \; Gr = \frac{g\beta_T (T_w - T_\infty){R_0}^3}{\nu^2}, \quad Gm = \frac{g\beta_C (C_w - C_\infty){R_0}^3}{\nu^2}, \; P_r = \frac{\mu C_p}{k_1}, \; P_e = R_e.P_r, S_c = \frac{\nu}{D_m}, \; Sr = \frac{D_m K_T (T_w - T_\infty)}{\nu T_\infty (C_w - C_\infty)}, \; K_c = \frac{K_0 \nu}{{u_0}^2}$

To consider the form of Caputo-Fabrizio fractional time model, equation (13) to equation (18) can be written in fractional derivative form as

$$D_t^\alpha u = B_0 + B_1 \cos(\omega t) + \frac{1}{R_e}\left(1 + \frac{1}{\beta}\right)\left(\frac{\partial^2 u}{\partial r^2} + \frac{1}{r}\frac{\partial u}{\partial r}\right) + A_0 Cos(Kt + \emptyset_0) - \frac{1}{D_a R_e} u - \frac{M^2}{R_e} u + \frac{Gr}{{R_e}^2}\theta + \frac{Gm}{{R_e}^2} C + \frac{sin\emptyset}{F} \tag{19}$$

$$P_e D_t^\alpha \theta = \left(\frac{\partial^2 \theta}{\partial r^2} + \frac{1}{r}\frac{\partial \theta}{\partial r}\right) + Nr\theta + P_e(Q_m + \theta_m) \tag{20}$$

$$R_e Sc \; D_t^\alpha C = \left(\frac{\partial^2 C}{\partial r^2} + \frac{1}{r}\frac{\partial C}{\partial r}\right) + Sr \; Sc \; \left(\frac{\partial^2 \theta}{\partial r^2} + \frac{1}{r}\frac{\partial \theta}{\partial r}\right) - S_c \, K_c \, R_e^2 C \tag{21}$$

With initial and boundary conditions are as,

$$u = \theta = C = 0 \; at \; t = 0, \forall r \in [0, 1] \tag{22}$$

$$\frac{\partial u}{\partial r} = \frac{\partial \theta}{\partial r} = \frac{\partial C}{\partial r} = 0, at \; r = 0, t > 0 \tag{23}$$

$$u = 0, \theta = 0, C = 0 \; at \; r = 1, t > 0 \tag{24}$$

Where, Caputo-Fabrizio operator is

$$D_t^\alpha u(r,t) = \frac{1}{1-\alpha}\int_0^t \exp\left(-\frac{\alpha(t-\tau)}{1-\alpha}\right)\frac{\partial u(r,\tau)}{\partial \tau}\; d\tau \tag{25}$$

The Laplace Transform of Caputo-Fabrizio operator Caputo and Fabrizio [12] can be express as

$$L\{D_t^\alpha u(r,t)\} = \frac{sL\{u(r,t) - u(r,0)\}}{(1-\alpha)\; s + \alpha} \tag{26}$$

With α $(0 < \alpha < 1)$ being the fractional order parameter.

2. Analytical Solution:

Taking the Laplace transform and Finite Hankel transform of order zero of equations (13) to (15) with initial and boundary conditions (16) to (18),

$$S^{\alpha}u(r,s) = -\frac{1}{R_e}\left(1+\frac{1}{\beta}\right)\left(\frac{\partial^2 u}{\partial r^2}+\frac{1}{r}\frac{\partial u}{\partial r}\right)-\frac{1}{D_a R_e}u-\frac{M^2}{R_e}u+A_0\left(\frac{S.\cos\emptyset_0 - K.\sin\emptyset_0}{K^2+S^2}\right)+\frac{B_0}{S}+\frac{B_1 S}{K^2+\omega^2}+\frac{G_r}{R_e^2}\theta+\frac{G_m}{R_e^2}C+\frac{\sin\phi}{S.F} \tag{27}$$

$$P_e S^{\alpha}\theta(r,s) = \left(\frac{\partial^2\theta}{\partial r^2}+\frac{1}{r}\frac{\partial\theta}{\partial r}\right) + Nr\theta + P_e\left(\frac{Q_m+\theta_m}{S}\right) \tag{28}$$

$$R_e S_c S^{\alpha}C(r,s) = \left(\frac{\partial^2 C}{\partial r^2}+\frac{1}{r}\frac{\partial C}{\partial r}\right)+S_r\,S_c\left(\frac{\partial^2\theta}{\partial r^2}+\frac{1}{r}\frac{\partial\theta}{\partial r}\right)-S_c\,K_c\,R_e^2 C \tag{29}$$

Where, $R_e = \frac{{R_z}^2}{\lambda v}$ is the Reynolds number, $D_a = \frac{\rho}{\lambda v}$ is a porosity parameter, R = $\frac{KN\lambda}{\rho}$ is the particle Concentration parameter, $Ha = \beta_0\sqrt{\lambda}\sqrt{\frac{\sigma \sin\theta}{\rho}}$ is the Hartman number, $F = \frac{R_0}{\lambda u_0 g}$ is the inclination angle parameter, $K_c = \frac{K_0 v}{{u_0}^2}$ the chemical reaction parameter, $\beta_1 = \frac{1}{R_e}\left[1+\frac{1}{\beta}\right]$.

The Boundary conditions (16) to (18) reduce to,

$$\frac{\partial u}{\partial r} = \frac{\partial\theta}{\partial r} = \frac{\partial C}{\partial r} = 0 \; at \; r = 0. \tag{30}$$

$$u = \theta = C = 0 \; at \; r = 1 \tag{31}$$

Applying Finite Hankel transformation of order zero in equations (27) and (28) with boundary condition (30) to (31) the following equation can be obtained.

$$\frac{1}{R_e}\left(1+\frac{1}{\beta}\right)[-r_n^2 u_H(r_n,s)] = \left[S^{\alpha}+\frac{1}{D_a R_e}+\frac{M^2}{R_e}\right]u_H(r_n,s)-\left[A_0\left(\frac{S.\cos\emptyset_0 - K.\sin\emptyset_0}{K^2+S^2}\right)+\frac{B_0}{S}+\frac{B_1 S}{S^2+\omega^2}+\frac{\sin\phi}{S.F}\right].\frac{J_1(r_n)}{r_n}-\frac{G_r}{R_e^2}\theta_H(r_n,s)-\frac{G_m}{R_e^2}C_H(r_n,s) \tag{32}$$

$$P_e\frac{S^2\,\theta_H(r_n,s)}{S+\alpha(1-s)} = -{r_n}^2\theta_H(r_n,s) - Nr\theta_H(r_n,s) + P_e\frac{Q_m+\theta_m}{S}.\frac{J_1(r_n)}{r_n} \tag{33}$$

$$R_e S_c S^{\alpha}C_H(r_n,s) = -{r_n}^2\theta_H(r_n,s)+(-{r_n}^2)\,S_r\,S_C\,\theta_H(r_n,s).\frac{J_1(r_n)}{r_n}-S_c\,K_c\,R_e^2 C_H(r_n,s) \tag{34}$$

Now, rearrange the equation (33)

$$\theta_H(r_n,s) = \frac{P_e\,(Q_m+\theta_m)}{S\left[r_n+P_e\frac{S}{S+\alpha(1-s)}\right]}\cdot\frac{J_1(r_n)}{r_n} \tag{35}$$

$$\theta_H(r_n,s) = \left[\frac{1}{S+B_{15}}B_{13}+\frac{1}{S-B_{15}}B_{14}\right]\frac{J_1(r_n)}{r_n} \tag{36}$$

$$C_H(r_n,s) = -\frac{S_r\,S_c\,r_n P_e\,(Q_m+\theta_m)}{\left(S\left[r_n+P_e\frac{S}{S+\alpha(1-s)}\right]\right)\left[\frac{R_e S_c\,.S}{S+\alpha(1-s)}+r_n+S_c\,K_c\,R_e^2\right]}\cdot\frac{J_1(r_n)}{r_n} \tag{37}$$

$$C_H(r_n,s) = \left(\frac{B_{29}}{S}+\frac{B_{30}}{S+B_{27}}+\frac{B_{29}}{S+B_{28}}\right).\frac{J_1(r_n)}{r_n} \tag{38}$$

$$\frac{1}{R_e}\left(1+\frac{1}{\beta}\right)[r_n^2]u_H(r_n,s)+\left[S^{\alpha}+\frac{1}{D_aR_e}+\frac{M^2}{R_e}\right]u_H(r_n,s) = -\left[A_0\left(\frac{S.\cos\emptyset_0-K.\sin\emptyset_0}{K^2+S^2}\right)+\frac{B_0}{S}+\frac{B_1S}{S^2+\omega^2}+\frac{\sin\phi}{S.F}\right].\frac{J_1(r_n)}{r_n}+\frac{G_r}{R_e^2}\theta_H(r_n,s)+\frac{G_m}{R_e^2}\,C_H(r_n,s) \tag{39}$$

Now, taking Inverse Laplace Transform and Inverse Finite Hankle transform of eqn. (36), (38) and (39), we get

$$\theta(r,t) = 2\,\sum_{n=1}^{\infty}\frac{J_0\left(\frac{r}{r_z}r_n\right)}{r_nJ_1^2(r_n)}\times\left[B_{13}e^{-B_{15}t}+\frac{B_{14}}{B_{15}}(1-e^{-B_{15}t})\right] \tag{40}$$

$$C(r,t) = 2\,\sum_{n=1}^{\infty}\frac{J_0\left(\frac{r}{r_z}r_n\right)}{r_nJ_1^2(r_n)}\times[B_{29}+B_{30}e^{-B_{27}t}+B_{31}e^{-B_{31}t}] \tag{41}$$

$$u(r,t) = 2\,\sum_{n=1}^{\infty}\frac{J_0\left(\frac{r}{r_z}r_n\right)}{r_nJ_1^2(r_n)}\times u_H(r_n,t)+Gr\,2\,\sum_{n=1}^{\infty}\frac{J_0\left(\frac{r}{r_z}r_n\right)}{r_nJ_1^2(r_n)}\times\theta_H(r_n,t)+Gm2\,\sum_{n=1}^{\infty}\frac{J_0\left(\frac{r}{r_z}r_n\right)}{r_nJ_1^2(r_n)}\times C_H(r_n,t) \tag{42}$$

The important characteristic for blood flow is the wall shear stress (skin friction), Nusselt Number and Sherwood Number can be expressed as,

$$C_f = -\frac{1}{R_e}\left(1+\frac{1}{\beta}\right)\left[\frac{\partial u}{\partial r}\right]_{r=1} \tag{43}$$

$$N_u = -\left[\frac{\partial\theta}{\partial r}\right]_{r=1} \tag{44}$$

$$S_h = -\left[\frac{\partial C}{\partial r}\right]_{r=1} \tag{45}$$

3. Results and Discussion

By analysing the effects of different parameter on blood and magnetic particle velocities, energy and concentration profiles, the numerical result is obtained and represent through the Fig. 2 to 13. Figure 2 to 3 show the effects of B_0 and B_1 on blood velocity where another parameter is fixed. In the process of increasing the parameters, it has been discovered that the blood flow is strengthened. When the pressure gradient is increased, the speed of the blood flow rises, which is a physical manifestation of this phenomenon.

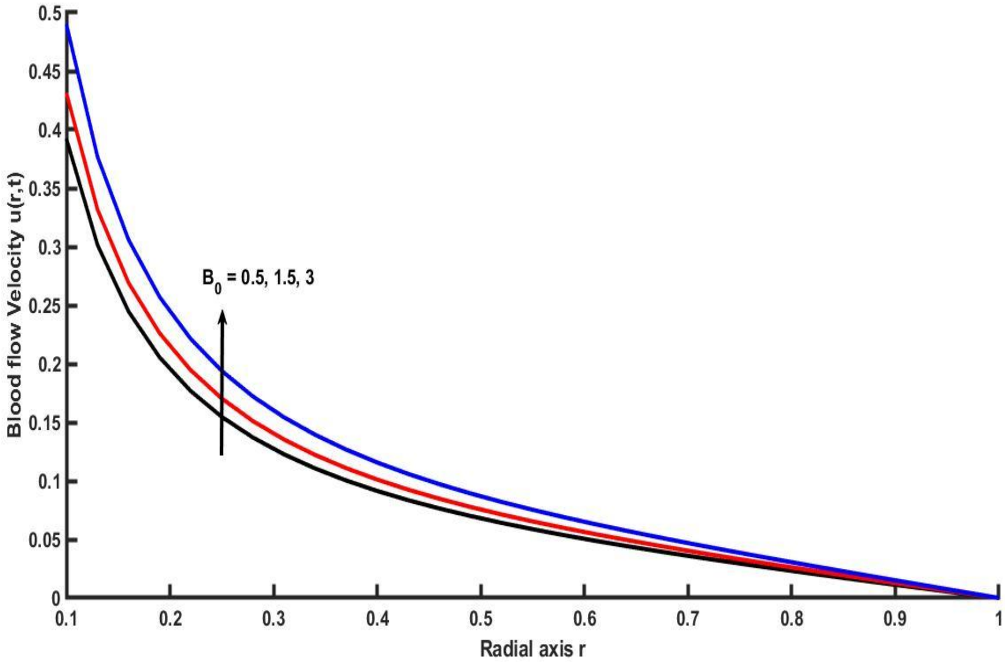

Fig. 2: B_0 on Blood flow Velocity

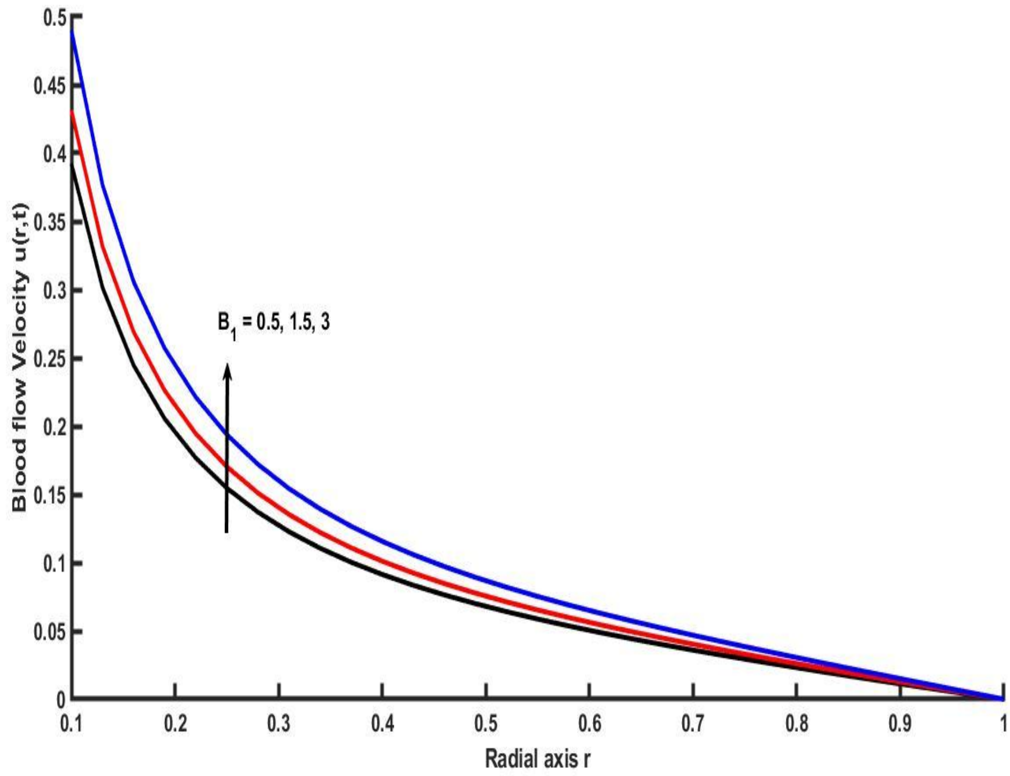

Fig. 3: B_1 on Blood flow Velocity

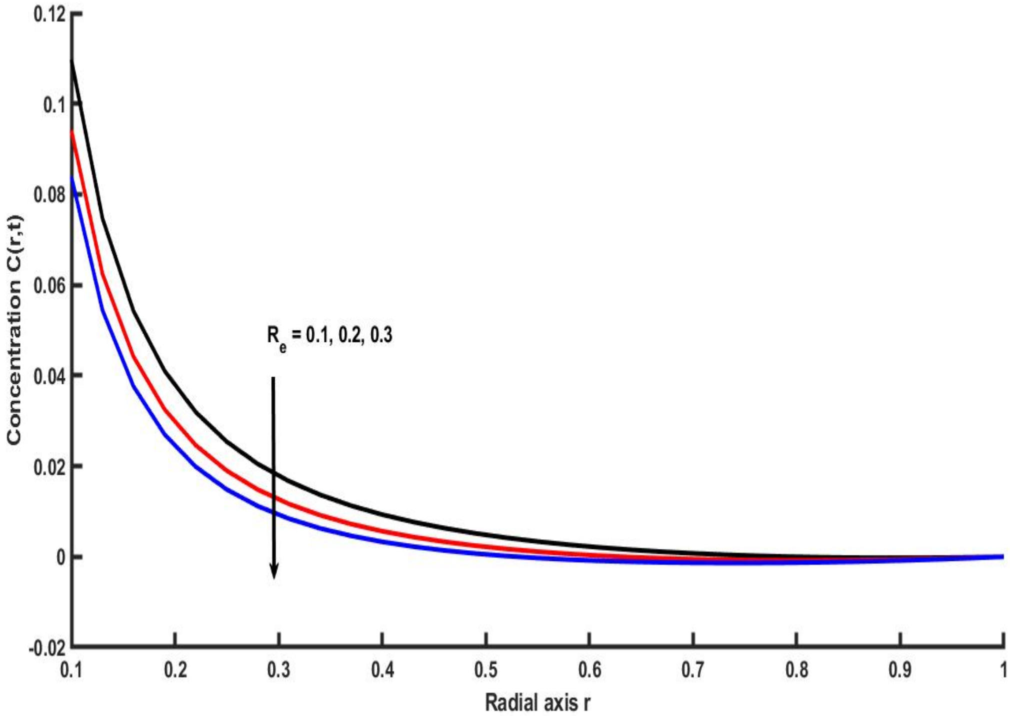

Fig. 4: R_e on Concentration

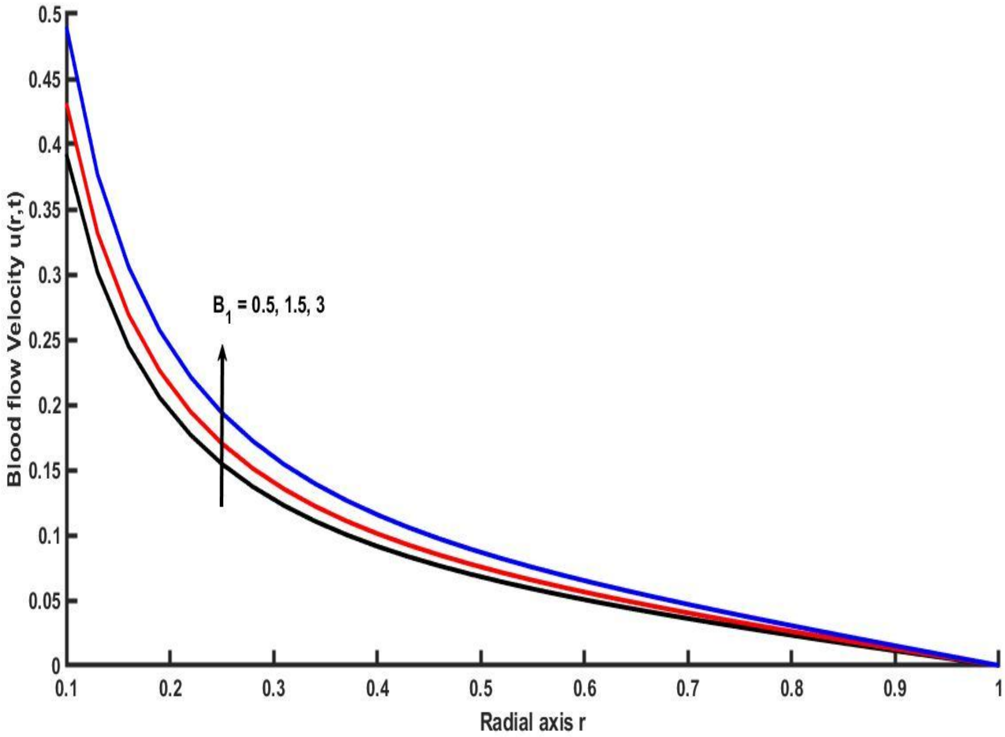

Fig. 5: β on Blood flow Velocity

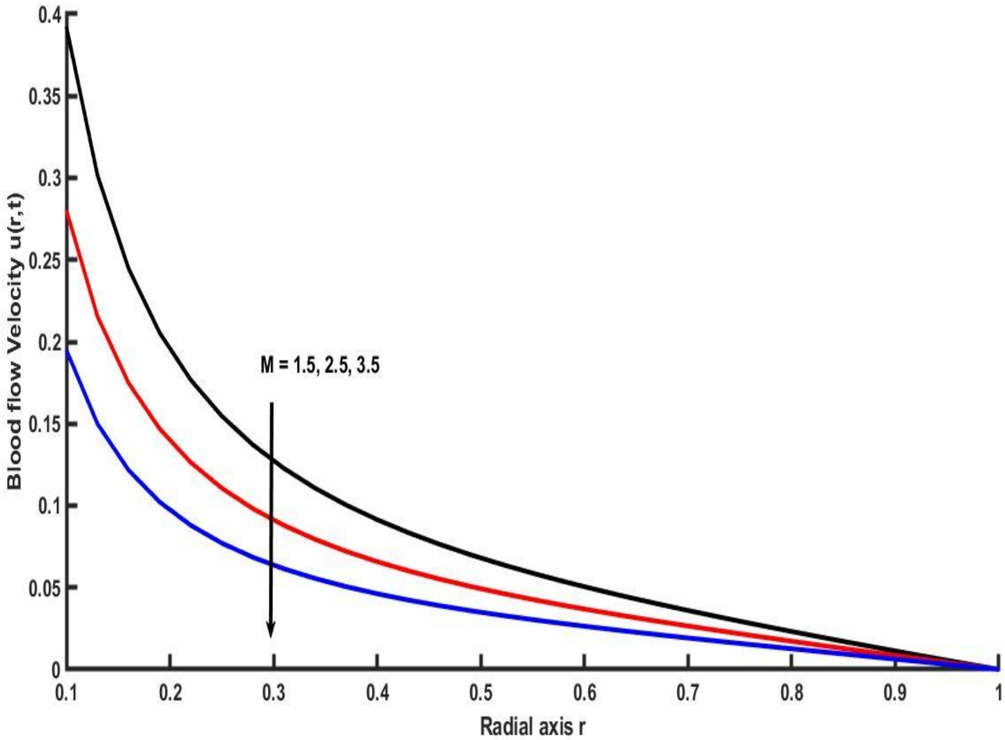

Fig. 6: M on Blood flow Velocity

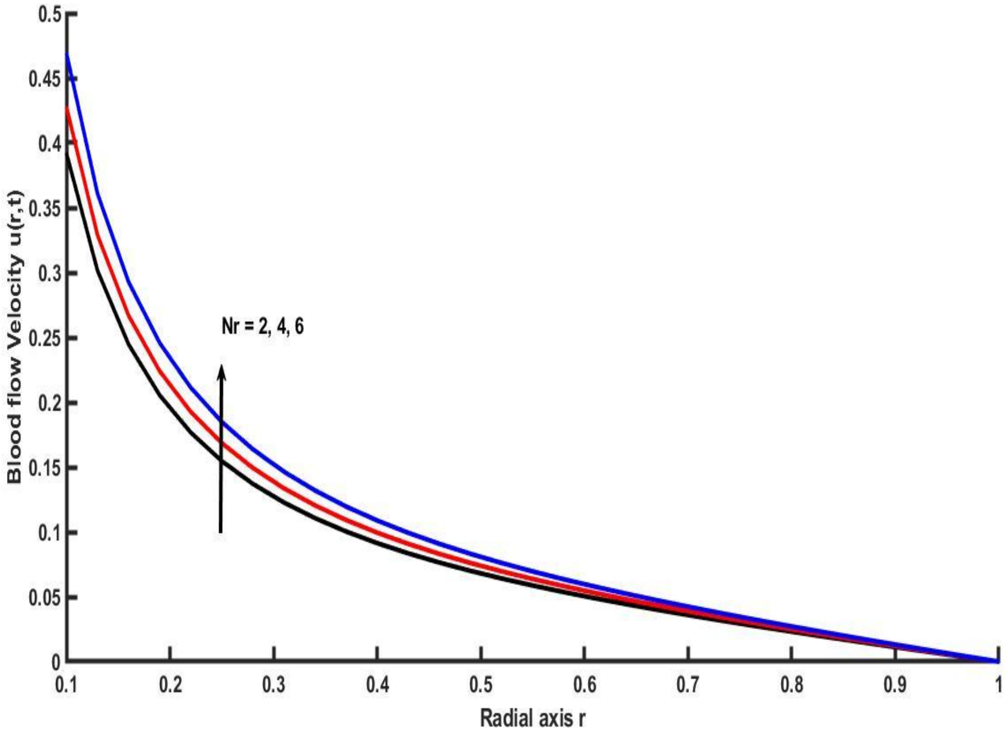

Fig. 7: Nr on Blood flow Velocity

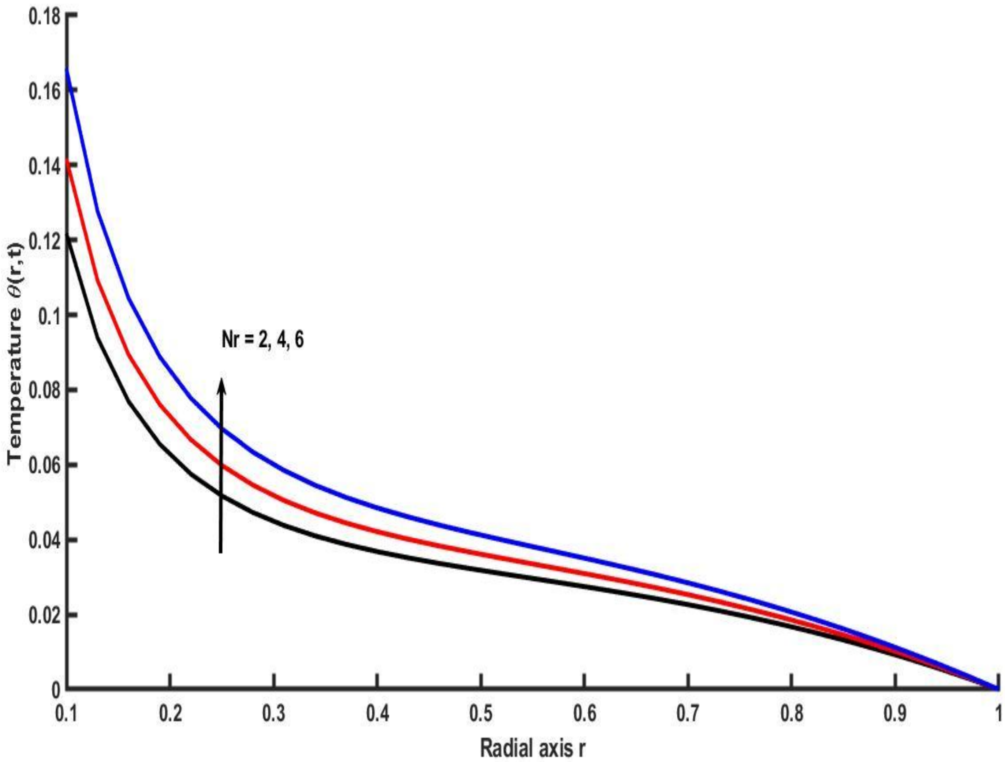

Fig. 8: Nr on Temperature

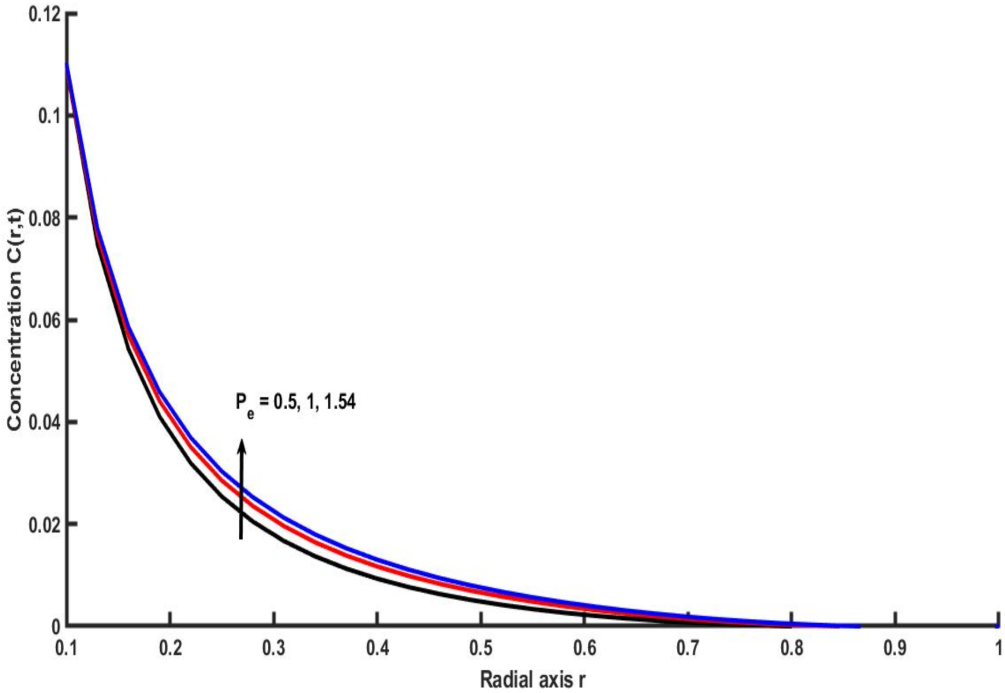

Fig. 9: P_e on Concentration

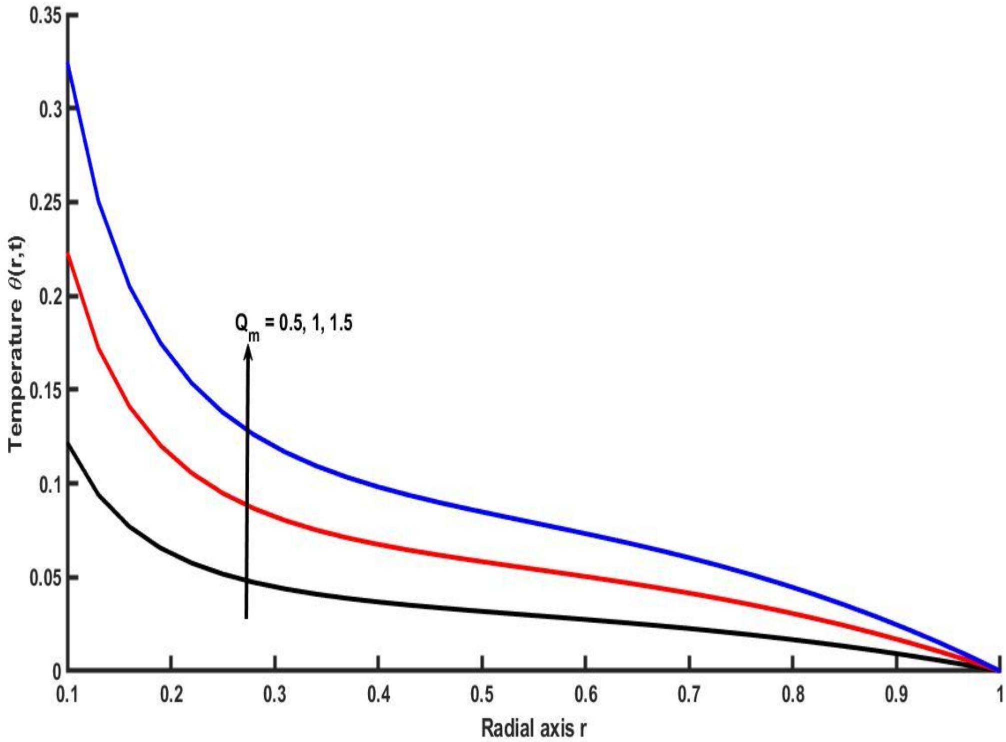

Fig. 10: q_m on Temperature

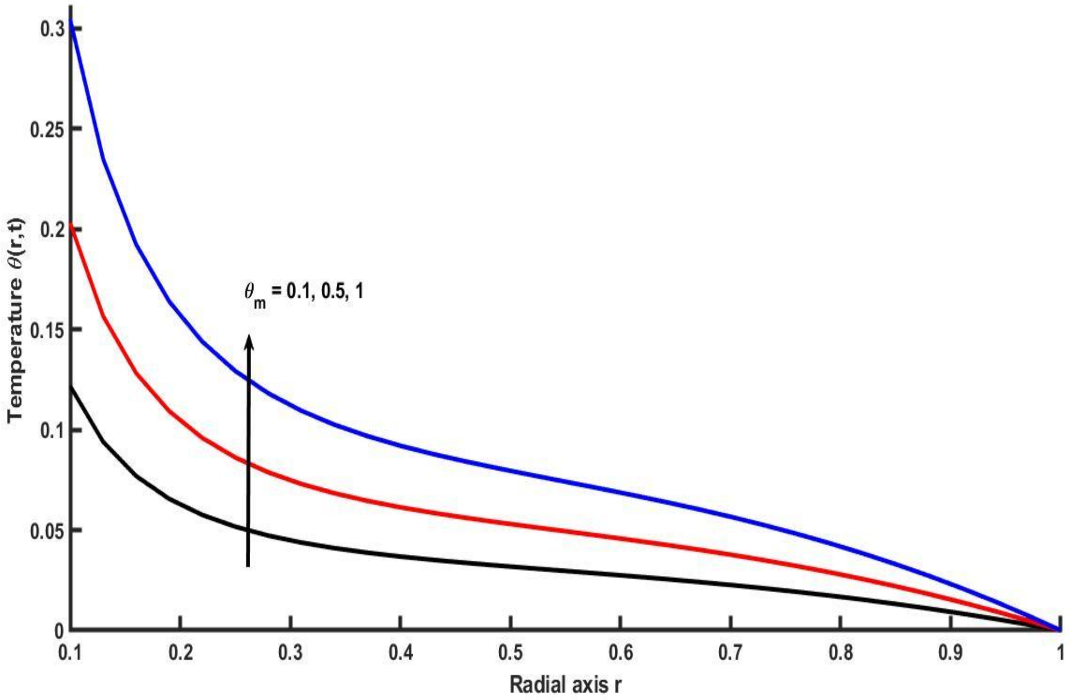

Fig. 11: θ_m on Temperature

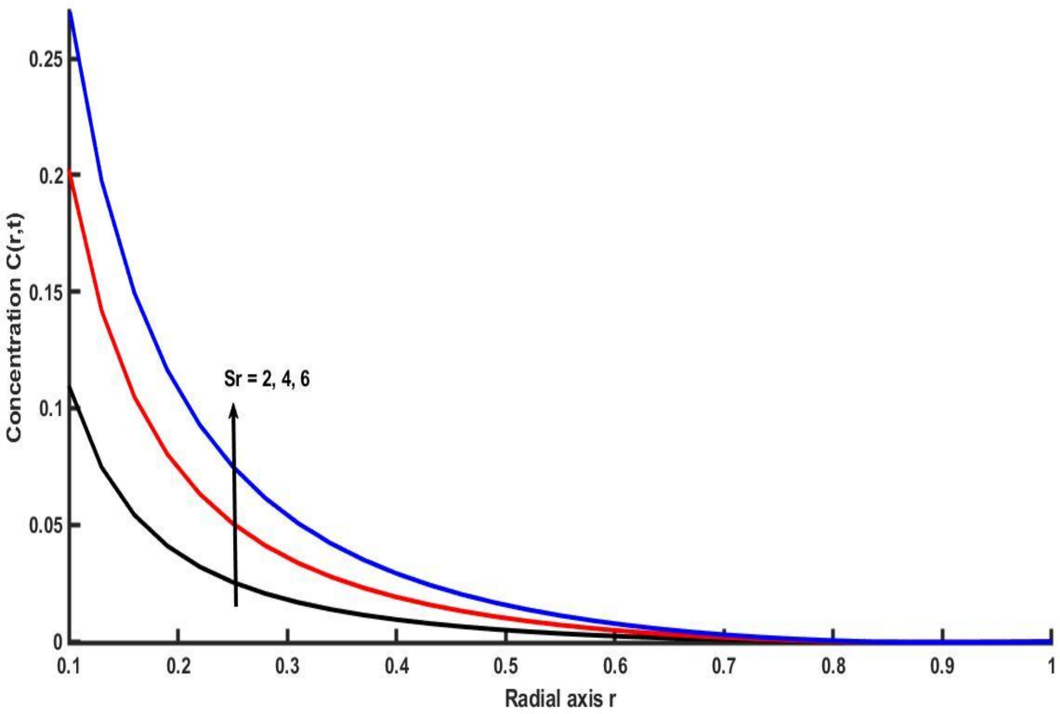

Fig. 12: S_r on Concentration

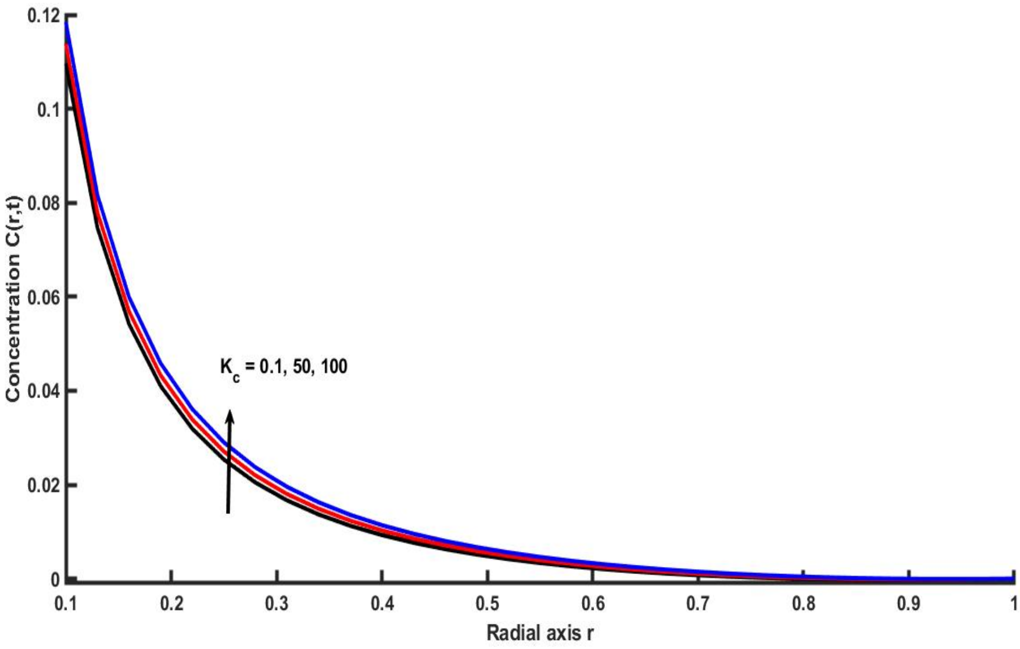

Fig. 13: Kc on Concentration

The influence of the Reynolds number, Re, on the concentration profiles is illustrated in Figure 4. When the Reynolds numbers are increased, it is observed that the velocity gradually drops. This has been observed. The influence that a single Casson fluid parameter has on velocity profiles is illustrated and discussed in Figure 5. Based on the findings, it can be deduced that the Casson fluid parameter has a tendency to speed up the flow of blood. Casson's behaviour is especially noteworthy in smaller arteries because of the risk of red blood cell spreading and collecting that occurs as a result of the rotation of the arterial axis. In Figure 6, we discuss the effects that an external magnetic field has on the mobility of fluids. The flow of motion is slowed down as a result of the effects provided by magnetic fields. A rotation of the charge particles would occur as a result of the magnetic field's impact. In addition to enhancing the Lorentz force, the magnetic field also has the effect of slowing down the standard flow rate.

Fig. 7-8 show the effects of thermal radiation parameter on velocity and temperature profiles respectively. Physically, when we increase the radiation fluid become thin, due to this reason temperature as well as velocity of flow is increase. This result is strongly agreed with real situation. The influence of the Peclet Number on the concentration profiles is illustrated in Figure 9. As can be observed, the mass transfer process becomes more complicated as the parameters increase. The influence of heat generation and absorption parameter on temperature profile is seen in Figures 10 and 11, respectively. A better heat transfer process is achieved as a result of an increase in heat. In light of the fact that increasing the value of heat generation causes the fluid to become thinner, these findings are consistent with the actual scenario. As a result, the fluid is accelerated more quickly. The thermos-diffusion effects on Concentration profiles discussed in Fig. 12. It is seen that the thermos-diffusion parameter improves the Concentration. The effects of Chemical reaction parameter on Mass transfer profiles are discussed through the Fig. 13. It is seen that the Mass transfer process improve with high values of chemical reaction parameter.

4. Conclusion:

Within the scope of this paper, the effects of radiation on Casson blood flow are investigated. The solution to the governing equations can be found by employing the Laplace transform method as well as the Hankel transform approach. After obtaining the data for velocity, temperature, and concentration, graphical representations of these values are created in order to facilitate a better understanding of their physics. The following are the most important findings from this research.

- The magnetic field element tends to slow down the speed of blood flow.
- A higher Peclet number indicates a higher blood concentration. This finding will be of interest to researchers studying the use of hyperthermia in cancer treatment.
- The Casson fluid parameter tend to improve the motion of the fluid.
- Both the systolic and diastolic pressure gradients have been shown to increase blood flow. These modifications may restore normal blood flow in the artery.
- The generation of heat and thermal radiation has a tendency to enhance both the process of heat transfer and the flow of blood.
- Mass transfer improve with high values chemical reaction parameter.

Appendix:

$$B_1 = R + Ha^2 + B_1 r_n^{\ 2}$$

$$B_2 = 1 + G - \alpha - R - R\alpha^2 + 2R\alpha + B_1 + B_1\alpha^2 - 2\alpha B_1 + GB_1 - G\alpha B_1$$

$$B_3 = \alpha + 2R\alpha^2 - 2R\alpha - 2B_1\alpha^2 + 2\alpha B_1 + G\alpha B_1$$

$$B_4 = B_1\alpha^2 - R\alpha^2, B_5 = 1 + \alpha^2 - 2\alpha + G + G\alpha\,,$$

$$B_6 = -2\alpha^2 + 2\alpha + G\alpha$$

$$B_7 = \frac{-B_3 \pm \sqrt{B_3^{\ 2} - 4B_2B_4}}{2B_2}, B_8 = \frac{-B_3 \pm \sqrt{B_3^{\ 2} - 4B_2B_4}}{2B_2},$$

$B_9 = \frac{{B_7}^2 B_5 + B_7 B_6 + \alpha^2}{B_7 - B_8}$,

$B_{10} = \frac{{B_8}^2 B_5 + B_8 B_6 + \alpha^2}{B_8 - B_7}$, $B_{11} = (r_n)(1-\alpha) + P_e$,

$B_{12} = (r_n).\alpha$

$B_{13} = P_e \frac{(Q_m + \theta_m)(1-\alpha)}{B_{11}}$, $B_{14} = P_e \frac{(Q_m + \theta_m).\alpha}{B_{11}}$,

$B_{15} = \frac{B_{12}}{B_{11}}$,

$B_{16} = -S_r S_c r_n P_e (Q_m + \theta_m)$, $B_{17} = r_n$,

$B_{18} = r_n + S_c K_c R_e^2$,

$B_{19} = R_e S_c$, $B_{20} = B_{17} - B_{17}\alpha + P_e$,

$B_{21} = B_{19} + B_{18} - B_{18}\alpha$, $B_{22} = B_{17}\alpha$

$B_{23} = B_{18}\alpha$, $B_{24} = \frac{B_{16}}{B_{20}.B_{21}}$, $B_{25} = 2\alpha(1-\alpha)$,

$B_{26} = (1-\alpha)^2$, $B_{27} = \frac{B_{22}}{B_{20}}$

$B_{28} = \frac{B_{23}}{B_{21}}$, $B_{29} = \frac{B_{24}(\alpha^2)}{B_{27}B_{28}}$, $B_{30} = \frac{B_{24}\left(\alpha^2 + B_{25}(-B_{27}) + B_{26}(B_{27})^2\right)}{(-B_{27})(B_{28} - B_{27})}$,

$B_{31} = \frac{B_{24}\left(\alpha^2 + B_{25}(-B_{28}) + B_{26}(B_{28})^2\right)}{(-B_{28})(B_{27} - B_{28})}$, $B_{32} = \frac{1-\alpha}{G-\alpha+1}$,

$B_{33} = \frac{\alpha}{G - \alpha + 1}$

$f * g -$ convolution of f & g , $f * g = \int_0^t f(z)g(t-z)dz$

Acknowledgement:

Authors are thankful to Ganpat University- Center for Advanced Research Studies (CARS) to provide financial support to carry research work

References:

[1] Casson, N., A flow equation for pigment oil suspensions of the printing ink type, in Rheology of Disperse Systems, edited by C.C. Mill (Pergamon Press, Oxford, 1959) pp. 84–102.

[2] Batchelor, Cx K., and George K. B., An introduction to fluid dynamics. Cambridge university press, 1967.

[3] Pramanik, S. "Casson fluid flow and heat transfer past an exponentially porous stretching Surface in presence of thermal radiation., Ain shams engineering journal 5, no. 1 (2014): 205-212. https://doi.org/10.1016/j.asej.2013.05.003.

[4] Bhattacharyya, K., Uddin, M. S., and Layek. G. C., Exact solution for thermal Boundary layer in Casson fluid flow over permeable shrinking sheet with variable wall temperature and thermal radiation. Alexandria Engineering Journal 55, no. 2 (2016): 1703-1712. https://doi.org/10.1016/j.aej.2016.03.010

[5] Mahanta, G., and Shaw. S., 3D Casson fluid flow past a porous linearly stretching sheet with convective boundary condition., Alexandria Engineering Journal 54, 3 (2015): 653-659. https://doi.org/10.1016/j.aej.2015.04.014.

[6] Ali, F., Khan, I., Samiulhaq, and Sharidan S., Conjugate effects of heat and mass transfer on MHD free convection flow over an inclined plate embedded in a porous medium., Plos one 8, no. 6 (2013): e65223. https://doi.org/10.1371/journal.pone.0065223

[7] Kataria, H.R., Patel, H. R., Singh, R. K., Effect of magnetic field on unsteady natural convective flow of a micropolar fluid between two vertical walls., Ain Shams Eng. J. 8 (1) (2017) 87–102, http://dx.doi.org/10.1016/j.asej.2015.08.013.

[8] Kataria, H. R., and Patel, H. R, Soret and heat generation effects on MHD Casson fluid flow past an oscillating vertical plate embedded through porous medium., Alexandria Engineering Journal 55, no. 3 (2016): 2125-2137. doi.org/10.1016/j.aej.2016.06.024

[9] Shukla, J. B., Parihar, R. S., Rao, B. R. P., and Gupta, S. P., Effects of peripheral layer viscosity on peristaltic transport of a bio-fluid, Journal of Fluid Mechanics 97, no. 2 (1980): 225-237. https://doi.org/10.1017/S0022112080002534

[10] Nadeem, S., Haq, R. U., Akbar, N.S., Khan, Z. H., MHD three- dimensional Casson fluid flow past a porous linearly stretch- ing sheet, Alex. Eng. J. 52 (4) (2013) 577–582. https://doi.org/10.1016/j.aej.2013.08.005

[11] Shehzad, S. A., Hayat, T., Alsaedi, A., Three-dimensional MHD flow of Casson fluid in porous medium with heat generation, J. Appl. Fluid Mech. 9 (1) (2016) 215–223. DOI: 10.18869/acadpub.jafm.68.224.24042

[12] Caputo, M., Fabrizzio, M., A new definition of fractional derivative with- out singular kernel, Prog. Fract. Differ. Appl. 1(2) (2015) 73-85. http://dx.doi.org/10.12785/pfda/010201

[13] Atangana, A., and Dumitru B, "New fractional derivatives with nonlocal and non-singular kernel: theory and application to heat transfer model." arXiv preprint arXiv:1602.03408 (2016).

[14] Sheikh, N. A., Farhad A, Muhammad S., Khan, I., Syed A. A., Ali S. A. and Metib S. Comparison and analysis of the Atangana–Baleanu and Caputo– abrizio fractional derivatives for generalized Casson fluid model with heat generation and chemical reaction." Results in physics 7 (2017): 789- 800. DOI: 10.1016/j.rinp.2017.01.025

[15] Maiti, S., Shaw S., and Shit, G. C., Caputo-Fabrizio fractional order model on MHD blood flow with heat and mass transfer through a porous vessel in the presence of thermal radiation, Physica A (2019), doi: https://doi.org/10.1016/j.physa.2019.123149.

[16] Jamil, D. F. et al., "Analysis of non-Newtonian magnetic Casson blood flow in an inclined stenosed artery using Caputo-Fabrizio fractional derivatives," Comput. Methods Programs Biomed., 203 (2021) 106044. doi: 10.1016/j.cmpb.2021.106044.

[17] Nakamura, M., and Tadashi S, Numerical study on the flow of a non- Newtonian fluid through an axisymmetric stenosis." (1988): 137-143. DOI: 10.1115/1.3108418

[18] Sud, V. K., and Sekhon, G. S., Flow through a stenosed artery subject to periodic body acceleration." Medical and Biological Engineering and Computing 25 (1987): 638-644. https://doi.org/10.1007/BF02447331

[19] Asjad, M. I., Karim, R., Hussanan, A., Iqbal, A., & Eldin, S. M. Applications of Fractional Partial Differential Equations for MHD Casson Fluid Flow with Innovative Ternary Nanoparticles. Processes, (2023) 11(1), 218. https://doi.org/10.3390/pr11010218

[20] Benmorsli, D., Fellah, Z. E. A., Belgroune, D., Ongwen, N. O., Ogam, E., Depollier, C., & Fellah, M., Transient Propagation of Longitudinal and Transverse Waves in Cancellous Bone: Application of Biot Theory and Fractional Calculus. Symmetry, (2022), 14(10), 1971. https://doi.org/10.3390/sym14101971

[21] Patel, Harshad and Nanda, Gopal, Utilization of Caputo Fractional Derivative in MHD Nanofluid Flow with Soret and Thermal Radiation Effects, Applications and Applied Mathematics: An International Journal (AAM), (2024) 19 (3) Article No. 7. https://digitalcommons.pvamu.edu/aam/vol19/iss3/7.

[22] Ramesh, K., & Devakar, M., Some analytical solutions for flows of Casson fluid with slip boundary conditions, Ain Shams Eng. J, (2015) 6(3), 967-975. https://doi.org/10.1016/j.asej.2015.02.007

[23] Akbar, N. S., Blood flow analysis of Prandtl fluid model in tapered stenosed arteries. Ain Shams Engineering Journal, (2014) 5(4), 1267-1275. https://doi.org/10.1016/j.asej.2014.04.014

[24] Kataria, H. R., & Patel, H. R., Effects of chemical reaction and heat generation/absorption on magnetohydrodynamic (MHD) Casson fluid flow over an exponentially accelerated vertical plate embedded in porous medium with ramped wall temperature and ramped surface concentration. Propulsion and Power Research, (2019) 8(1), 35 -46. https://doi.org/10.1016/j.jppr.2018.12.001

[25] Mittal, Akhil; Patel, Harshad; Patoliya, Ramesh; and Gohil, Vimalkumar (2024). Effects of Magnetic Field and Chemical Reaction on a Time Dependent Casson Fluid Flow, Applications and Applied Mathematics: An International Journal (AAM), (2024), 19 (3), Article 8. https://digitalcommons.pvamu.edu/aam/vol19/iss3/8